Thermal volatilisation analysis of graphite intercalation compound fire retardants

Kellie Muir[1] · John J. Liggat[1] · Luke O'Keeffe[2]

Abstract

Thermally expandable graphites are becoming increasingly popular as intumescent fire retardants for polymeric systems due to their excellent thermal and barrier properties. Therefore, it is important to understand their thermal degradation pathways and monitor products for any that may be toxic or affect the stability of the polymer. Here, two commercially available thermally expandable graphites with different intercalated acids have been analyzed using thermal volatilisation analysis—sub-ambient distillation (TVA-SAD), mass spectrometry (MS) and Fourier transform infrared spectroscopy (FTIR). Results confirm the presence of three principal thermal events relating to the expansion of graphite nitrate and graphite bisulfate. Isothermal analyses provide a deeper understanding of the processes and decomposition products released from each stage. For both graphites, desorption of migrating gases and volatilisation of water occur in the first instance. Graphite bisulfate releases CO_2, CO, and water upon expansion and releases a significant volume of SO_2 subsequently. Graphite nitrate expansion proceeds with the release of NO_2, NO, CO and water. Additionally, the release of non-condensable species and carbonyl-derived fragments suggests that the exfoliation process occurs by multiple different degradation processes. For expansion to occur, sufficient pressure must be produced in the graphite interlayer spacing; this is achieved by volatilisation of intercalated species and by the decomposition of functional groups on the outer edges and basal planes created from the oxidation of graphite.

Keywords Expandable graphite · Evolved gas analysis · Thermal analysis

Introduction

Carbon exists in many different allotropes displaying various molecular structures with unique properties. At atmospheric pressure and temperature, graphite is the most stable type of carbon allotropes and is widely utilised across various industries, particularly in the form of graphite intercalation compounds (GICs) [1]. GICs can be obtained by the insertion of small molecules or ions in between one or several connecting stacked parallel layers of graphene, with the number of graphene layers in between an intercalated layer referred to as the stage number. This can be achieved via several methods including liquid or electrochemical intercalation [2].

Some GICs are used to obtain thermally expandable graphite (TEG) which, when exposed to elevated temperatures, can expand up to several hundred times forming a carbonaceous low density, porous material with high thermal stability and electric conductivity [3].

Thermally expandable graphite has been utilised as an intumescent type flame retardant in polymeric coatings and is widely used in polyurethane foams in the automotive and air industry [4]. Unlike traditional intumescent systems, it can function as a self-expanding system and has been proven to effectively improve the fire retardancy of polymeric materials [5, 6]. As a fire retardant, expandable graphite functions primarily in the condensed phase forming a stable insulating char layer when exposed to increased temperatures. This char layer limits heat and mass transfer between the flame and material thereby reducing oxygen diffusion and subsequently interrupting the combustion process.

The formation of TEG occurs typically through a two-stage intercalation process involving GICs embedded with Brönsted acids, most commonly nitric or sulfuric acid
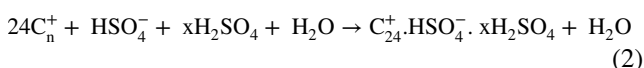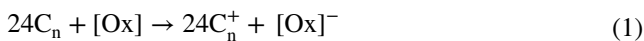
✉ John J. Liggat
  j.j.liggat@strath.ac.uk

1 Department of Pure and Applied Chemistry, University of Strathclyde, Glasgow G1 1XL, Scotland, UK

2 Abesco Fire Ltd, Alma Place, Laurencekirk, Aberdeenshire AB30 1AL, Scotland, UK
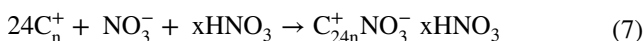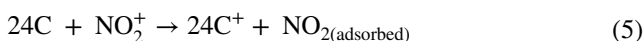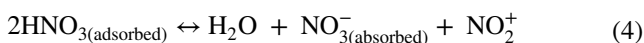
although a greener route to their production using sodium carbonate has recently been disclosed [7].

However, secondary intercalation acids may also be used to increase the level of oxidation. The graphite is then washed commonly with water and/or acid to form the final complex, termed graphite nitrate or graphite sulfate, depending on the intercalation acid used [8]. The intercalation chemistry of GICs has been studied fairly extensively [9–12]. Reactions 1–2 represent the chemical intercalation process for graphite bisulfate ($C_{24}^+ HSO_4^- .2H_2SO_4$):

$$24C_n + [Ox] \rightarrow 24C_n^+ + [Ox]^- \tag{1}$$

$$24C_n^+ + HSO_4^- + xH_2SO_4 + H_2O \rightarrow C_{24}^+.HSO_4^-. xH_2SO_4 + H_2O \tag{2}$$

In the presence of sulfuric acid and an oxidising agent (Ox), commonly potassium permanganate or nitric acid, natural graphite flake (C_n, where n is the stage number) may be oxidised (reaction 1). The positively charged graphite structure provides favorable conditions for intercalation via electrostatic attraction of acid anions. The resultant product is a graphite acid salt, ionic in nature due to the balance in charge between the positively charged graphite and negatively charged acid anions (reaction 2). Residual molecules of acid are also included in the structure [13]. An early X-ray study by Rodorf [14] showed that this intercalation process results in an increase in *d*-spacing between the parallel layers of graphene resulting in a two- to threefold increase along the c-axis of graphite.

Graphite nitrate, $C_{24n}^+ NO_3^-. xHNO_3$ can be prepared similarly to graphite bisulfate. However, intercalation occurs spontaneously due to the strong oxidising behavior of nitric acid. Forsman et al. [12] represented the formation of graphite nitrate with 96% nitric acid with the following sequence of reactions:

$$HNO_{3(g)} \rightarrow HNO_{3(adsorbed)} \tag{3}$$

$$2HNO_{3(adsorbed)} \leftrightarrow H_2O + NO_{3(adsorbed)}^- + NO_2^+ \tag{4}$$

$$24C + NO_2^+ \rightarrow 24C^+ + NO_{2(adsorbed)} \tag{5}$$

$$NO_{2(adsorbed)} \rightarrow NO_{2(g)} \tag{6}$$

$$24C_n^+ + NO_3^- + xHNO_3 \rightarrow C_{24n}^+ NO_3^- xHNO_3 \tag{7}$$

Reaction 4 shows the absorbed-phase reaction in which the nitronium ions are generated from the dissociation of nitric acid. These electrophilic nitronium ions can then withdraw electrons from the graphite, rendering the graphite positive and then desorbing as NO_2 (reactions 5, 6). The

positively charged graphite can then attract nitrate ions and HNO_3 molecules creating an electronically neutral graphite nitrate salt (7).

It is believed that during thermal expansion, the interplanar attractions between layers of intercalated graphite are weakened as pressure increases due to the vaporisation of intercalated products and residual water inserted in the washing process [1]. Expansion occurs when enough internal pressure has been produced to break Van der Waals attractions, the intercalate is vaporised or decomposed and the GIC rapidly increases in volume along the c-axis resulting in the formation of worm-like carbon particles and the release of desorbed gases [15]. The exfoliation process is still not completely understood, although has been reported to occur in two stages, the first involving the slow migration of intercalant to the outer surface of the graphite and secondly the rapid expansion attributed to the boiling of products still trapped within the graphitic structure [8]. Furdin [8] reported correspondence between the boiling point of the free intercalate molecule and expansion temperatures of both graphite nitrate and graphite bisulfate. With H_2SO_4 and its dehydrated form SO_3, the boiling temperature is above that of expansion. Therefore, in this case, an increase in internal pressure sufficient for exfoliation may be explained by subsequent reactions between the intercalant and graphite to produce gaseous species.

The thermal decomposition of intercalates and their reaction with graphite to create thermal expansion has been reported. Camino et al. [16] proposed a redox reaction between H_2SO_4 and graphite to be responsible for creating the blowing gas to allow exfoliation in graphite bisulfate:

$$C + 2H_2SO_4 \rightarrow CO_{2(g)} + 2H_2O_{(g)} + 2SO_{2(g)} \tag{8}$$
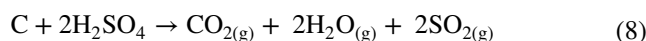
Camino et al. reported the major mass loss of TEG to occur between 200 and 350 °C, with expansion beginning at 200 °C. According to this reaction, the intercalated acid and graphite react during expansion which starts with the release of H_2O, CO_2, and SO_2.

Saidaminov et al. [11] observed a two-stage gas emission when heating graphite nitrate from 50 to 900 °C under inert conditions. In the first stage, which occurred between 80 and 150 °C, NO_2 and CO were observed. These were attributed to the decomposition of solvated HNO_3 to NO_2, O_2, and H_2O, resulting in the immediate oxidation of the graphite to form CO. The second stage, occurring between 150 and 250 °C, resulted in the formation of NO, NO_2 and CO. These gases were believed to be formed by the decomposition of intercalated nitrate anions resulting in exfoliation of the graphite particles.

It has also been suggested that oxidation may occur more readily in the flaws of the graphite structure, producing highly oxidised segments, similar to graphite oxide [17].

The structure of graphite oxide has been studied extensively and is reported to contain a variety of functional groups including carbonyl, carboxyl, epoxy, phenol, quinone, and anhydrides [10, 18]. Water is also a dominant feature in the structure of graphite oxide and has been reported to form hydrogen bonds with epoxide groups creating strong interactions to the basal plane [10]. Under thermal conditions, these groups decompose to CO_2, CO, and water is released, causing the expansion of the graphite oxide [18]. Therefore, it is possible that the volatilisation of these groups on basal planes and periphery also contributes to the expansion of graphite bisulfate and graphite nitrate.

Thus, Peng et al. [19] deliberately introduced oxygen-containing groups on the edge and inner layers of natural flake graphite using $KMnO_4$, and $HClO_4$ as the oxidative agents with NH_4NO_3 as a co-reagent, in a successful attempt to generate a low-temperature TEG. Interlayer spacing increased upon oxidation without perturbing the inner hexagonal structure. The effect of edge oxidation on the spacing was thought to be critical—too little and the spacing did not increase sufficiently for intercalation of the $KMnO_4$, $HClO_4$ and NH_4NO_3 to occur; too much and the intercalation agent was insufficiently constrained. In both cases, expansion was sub-optimal. When optimised, expanded volumes in excess of 400 mL g^{-1} could be achieved.

Of course, critical to the performance of the TEG is its ability to be dispersed throughout the polymer matrix without detriment to the properties of the polymer in normal service. Few studies include this as a factor, although recently Tayfun et al. have reported on the effect of the incorporation of TEG at 10–20% on ABS [20]. While elongation to break and impact strength are reduced, tensile strength and modulus increase, while UL-94 rating improves from NR to V1. For rigid polyurethanes foams, Wang et al. have developed core–shell expandable graphite@aluminum hydroxide additives which are effective fire retardants but also disperse well without destroying the cell structure [21].

While effective as fire retardants, TEGs are by no means perfect. While their effectiveness depends on their mode of action is as a low density thermal barrier, this low density of makes it susceptible to being blown away by turbulent airflows at the fire front, rendering it ineffective. Like many fire retardants, expandable graphites can lead to excessive smoke generation. Hence, hybrid systems have been investigated to address these shortcomings. Most recently, Wang et al. have demonstrated that hybrid expandable graphite-double layer hydroxides are very effective fire retardants for poly(vinyl alcohol). By generating a dense and robust char layer, not only can they reduce peak heat release rates by as much as 50% relative to PVA or simple PVA-EG formulations, but smoke density also drops by as much as 66% [22].

A recent keyword analysis tracking the evolution of research into fire retardant rigid polyurethane foams revealed that the most frequent keyword is "expandable graphite" [23]. Understanding the thermal decomposition behavior and decomposition products of TEGs is therefore extremely important, particularly concerning its use as a fire retardant, as it is vital to monitor the release of gases that may be toxic or affect nearby infrastructure (the release of acids from burning cables is a known source of damage to electronic equipment) or which may adversely affect the stability of the polymer matrix. Yet despite the many papers on the TEGs and the exfoliation process of GIC, few focus on volatile release. In this paper, we focus on the thermal decomposition of expandable graphites containing sulfuric acid and nitric acid by the unique evolved gas analysis technique thermal volatilisation analysis (TVA). The main objective of this work is to provide real-time analysis of decomposition products occurring during exfoliation to determine a detailed mechanism of action for the expansion process. Using TVA, evolved gases can be separated and characterised by Fourier transform infrared spectroscopy (FTIR) and mass spectrometry (MS) providing an in-depth analysis at the significant temperatures during exfoliation and therefore an understanding of decomposition chemistry occurring.

Experimental

Materials

Two commercially available expandable graphites were used for this research: FireCarb TEG 500 (LKAB Minerals), a GIC containing sulfuric acid and Nord-min KP251 (Nordmann), a GIC containing nitric acid.

Thermal Volatilisation analysis

All TVA analyses were performed on a TVA line which was built in-house, based upon the principles described by McNeill [24].

The apparatus consists of a sample chamber and programmable tube furnace connected to a continuous glass line with four parallel limbs which are constantly pumped to a vacuum of around 10^{-4} mbar by an oil diffusion pump and a rotary pump. Four cryogenic traps cooled by liquid nitrogen at a temperature of − 196 °C are placed on each parallel limb and another two are present just upstream of the sample and next to the diffusion pump.

Six Pirani gauges in total are used to monitor changes in pressure, these are placed before and after the primary cold trap and after each cold trap on the parallel limbs.

Products that are volatile at the degradation temperature but not at ambient temperature are collected at the top of the sample tube utilising a water-filled cold ring which is placed around the top of the tube. Other volatiles that are volatile

at both degradation and ambient temperatures are further separated into those that are condensable at − 196 °C and those which are not.

Condensable gases are collected in the primary cold trap, monitored by a change in pressure detected by the first Pirani gauge. Non-condensable products pass through the cold trap and are detected by the second Pirani gauge. Measurements from the Pirani gauges and the thermocouple are collected producing a TVA curve that shows the evolution of volatiles as a function of temperature and time.

Trapped, low-boiling species can be distilled into separate secondary cold traps by slowly heating the primary sub-ambient trap to ambient temperatures, again monitored by Pirani gauges, and recorded as a function of trap temperature as they move to the secondary traps. Degradation products can be characterised by MS as they evolve or by subsequent distillation into gas cells to be analyzed by FTIR.

All dynamic TVA analyses were conducted under vacuum using ~ 200 mg samples, heated from ambient temperatures to 575 °C at a rate of 20 °C min^{-1}. For isothermal TVA experiments, a 200 mg sample was heated at a ramp of 20 °C min^{-1} and held isothermally for approximately 30 min. The same sample was then allowed to cool to ambient temperatures before heating to the next isothermal temperature. For graphite bisulfate, isothermal experiments were conducted at 125, 190, 275, and 575 °C. For graphite nitrate, isothermal analyses were conducted at 145, 245, 350, and 575 °C. The temperatures were chosen based on thermal events identified from the dynamic TVA analysis. Volatile products were monitored continuously as they are distilled from the cold trap using a 1–300 amu Hiden single quadruple RGA mass spectrometer. Depending on the volume of products released, volatiles were separated into one to four fractions. The SAD products were collected into vacuum-tight gas cells with sodium chloride windows and characterised by FTIR spectroscopy. All FTIR spectroscopy was performed on a PerkinElmer Spectrum 100 FTIR spectrometer used in transmission mode with a resolution of 4 cm^{-1} and 16 scans. A small camera was also mounted at the base of the sample tube to monitor the expansion of graphite throughout the experiments.

Results and discussion

Thermal expansion of graphite bisulfate

Dynamic thermal volatilisation analysis

The dynamic TVA profile (Fig. 1) shows the volatile release profile associated with the thermal expansion of graphite bisulfate under vacuum as a function of sample temperature.
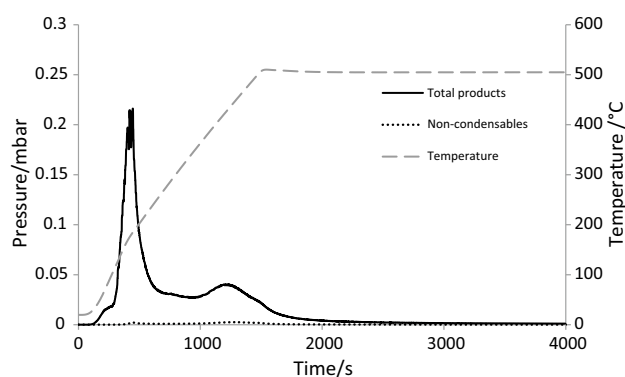

Fig. 1 Dynamic TVA degradation profile for the thermal expansion of graphite bisulfate

Table 1 Temperatures for the main thermal events occurring in the expansion process for graphite bisulfate

Degradation peak	Onset of evolution of volatiles /°C	Maximum evolution of volatile /°C	End of volatile evolution /°C
Peak 1	75	96	125
Peak 2	133	190	275
Peak 3	350	437	575

The sample temperatures for each key thermal event are summarised in Table 1.

It can be observed from the TVA curve that three main thermal events are occurring. Visual observations of the sample tube and video footage reveal that peak 2 is associated with the main exfoliation event. This is consistent with the expansion temperature reported by Camino et al. [16]. Peak 3 is consistent with the thermal decomposition of H_2SO_4 according to reaction (9) [25]:

$$H_2SO_4 \rightarrow SO_3 + H_2O \tag{9}$$

Sub-ambient distillation and characterisation

The condensable fraction collected from the decomposition of the graphite flake was separated into three fractions, and the resulting sub-ambient curve is presented in Fig. 2. Furthermore, each condensable fraction was characterised by MS and FTIR. In a separate experiment, non-condensable products were also characterised by MS and found to consist predominately of CO. MS analyses are displayed in Figs. 3 and 4 and FTIR spectra are presented in Fig. 5. Product identification is presented in Table 2.

The volatiles produced correspond to the redox reaction (8) proposed by Camino et al. [16] although H_2O is observed in proportionally large volumes compared to CO_2 and SO_2.

Fig. 2 SAD curve for the condensable fraction collected from the dynamic TVA run for graphite bisulfate
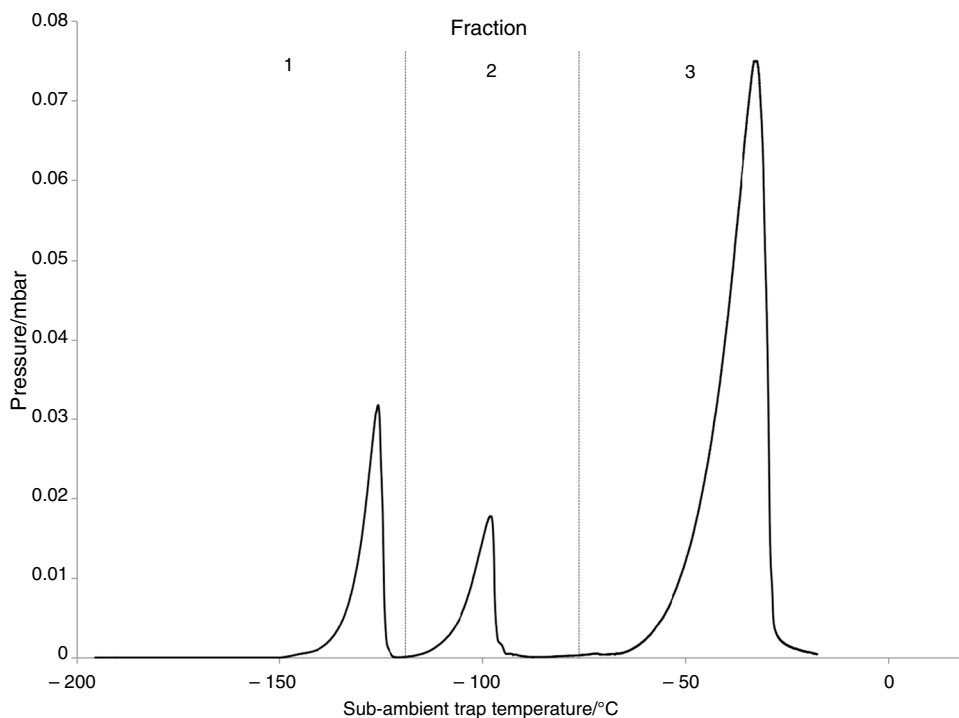
Water may be involved in the expansion process as a blowing agent due to the evaporation of intercalated molecules bound within the interplanar layers of the graphite, increasing the distance between stacked layers of graphite. Analyses also reveal CO_2 as a major product. The presence of CO_2 may be attributed to over-oxidation of flaws in the graphite structure as suggested by Focke et al. [17], creating heavily oxidised pockets of graphite that produce CO_2 as exfoliation temperatures are reached. Over-oxidation of graphite bisulfate can result in the formation of graphite oxide meaning a combination of both may be present. Furthermore, the presence of CO in the non-condensable products in the TVA curve above 200 °C may be a consequence of graphite oxide as it decomposes above 200 °C to create CO, CO_2, and H_2O [26]. Also, according to Yakovlev et al. [27], if over-oxidation of graphite bisulfate occurs, water will also be oxidised to oxygen, also generating O_2, CO, and CO_2.

Isothermal thermal volatilisation analysis

To further examine the degradation chemistry occurring, isothermal experiments were performed to capture the volatiles produced from each main thermal event. Sequential isothermal experiments were conducted at 125, 190, 275, and 575 °C, and the evolved gases were characterised by FTIR and MS. The sequential TVA and SAD curves are presented in Figs. 6 and 8 respectively. Identified products are listed in Table 3.

The curves show that the largest volume of volatiles produced is at 190 °C as the Pirani gauges record a maximum pressure of approximately 0.12 mbar. This corresponds to an increase in pressure between graphene layers, consequently overcoming the interplanar attractions and inducing the onset of exfoliation, which according to Chung et al. [9] is a result of the vaporisation of intercalated species. When exfoliation temperatures are reached, around 190 °C, expansion proceeds rapidly accompanied by the production of non-condensable species. The appearance of non-condensable products at this stage reveals that CO has now been formed, and this may be explained by the presence of graphite oxide as it decomposes to produce CO and CO_2. Finally, to complete the isothermal analysis, the furnace temperature was increased to 575 °C. At this final temperature, a relatively large volume of total products and non-condensable products are still being produced. The largest volume of SO_2 is produced in this final isothermal step. It is possible that since exfoliation has occurred, free molecules of sulfuric acid previously held within the graphite matrix have been released and continue to volatilise and decompose.

Isothermal sub-ambient distillation and characterisation

At 125 °C, FTIR and MS analyses confirm water as the volatile species collected, likely due to the evaporation of residual water used in the intercalation process. At 190 °C, the largest volume of volatiles is produced according to increased pressure detected by the Pirani gauges, and these include H_2O, CO_2, and trace levels of SO_2. At this stage in
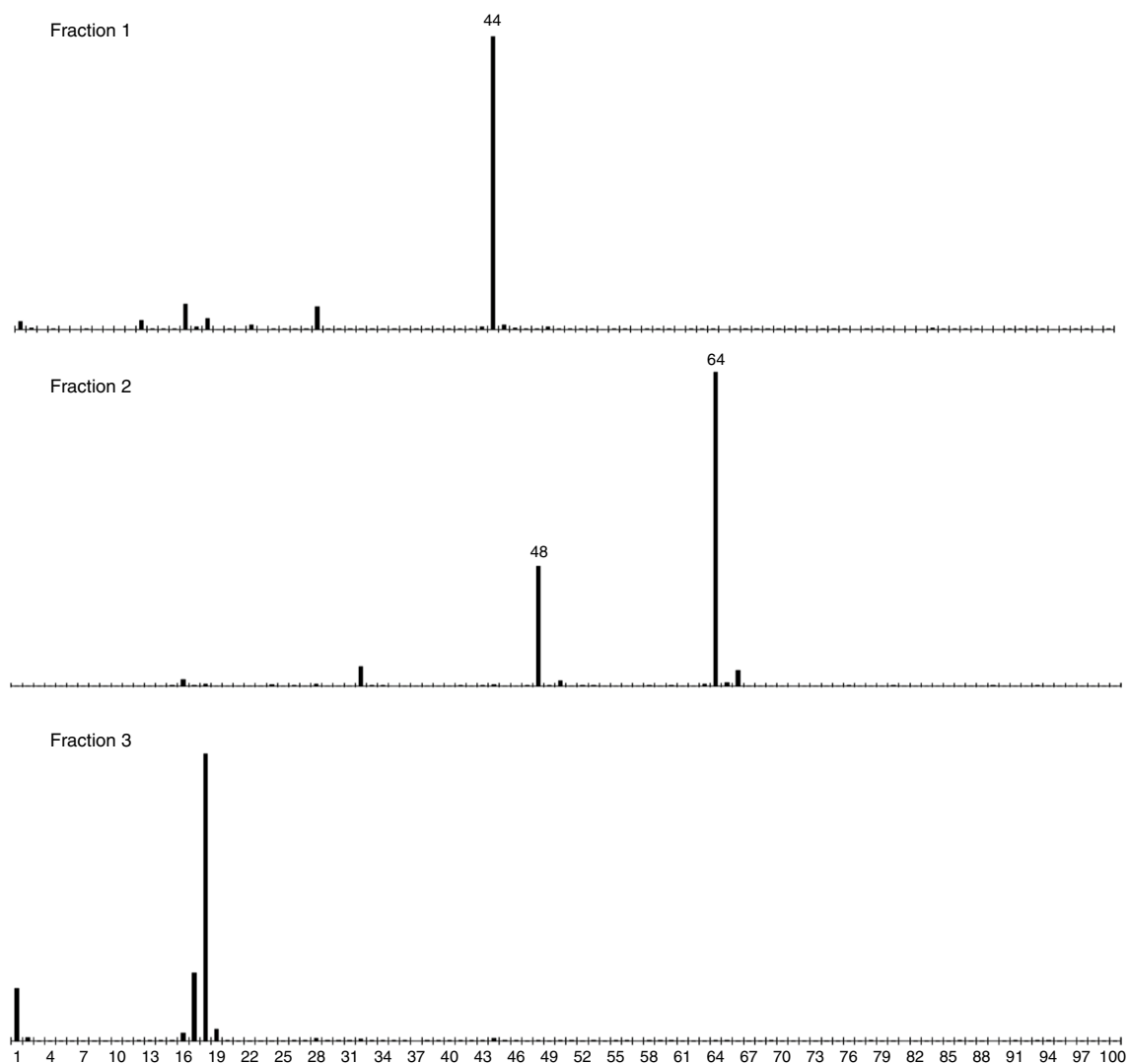
Fig. 3 MS of the condensable products from SAD fractions 1–3 from the dynamic TVA run for graphite bisulfate showing CO_2 (fraction 1), SO_2 (fraction 2) and H_2O (fraction 3)
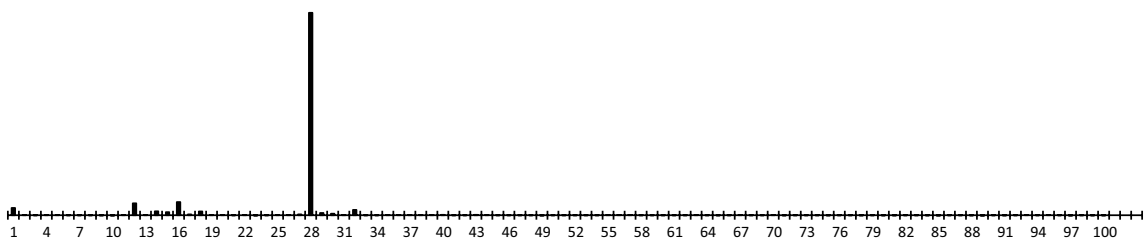

Fig. 4 MS of the non-condensable products from the dynamic TVA run for graphite bisulfate showing CO as the dominant product

the process desorption of gases is occurring, internal pressure is building and d-spacing is increasing due to the evaporation of volatile products generated by decomposition reactions. Focke et al. [17] proposed that during the intercalation process, due to the disordered and flawed nature of graphite

flake, heavily oxidised flawed regions of graphite oxide type material may be produced. Jimenez et al. [26] describe the thermal decomposition of graphite oxide to firstly occur with a dehydration step releasing water and a decomposition stage in which CO_2, CO, and water are evolved. These processes
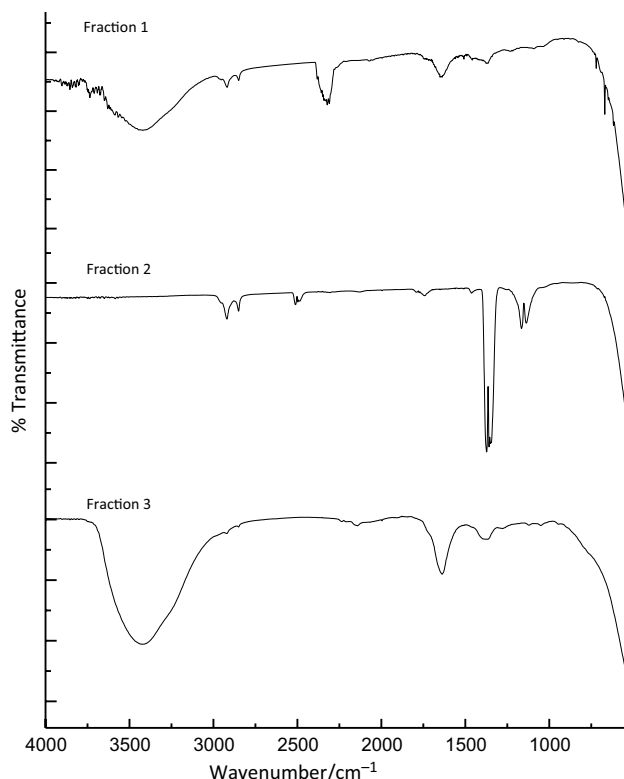
Fig. 5 FTIR gas phase spectra of the volatile SAD products in fractions 1–3 from the dynamic TVA for graphite bisulfate showing CO_2, SO_2, and H_2O, respectively

**Table 2** Characterisation of products from the dynamic TVA run of graphite bisulfate

Fraction	Fraction range /°C	Condensable products
1	− 200 to − 138	CO_2
2	− 138 to − 68	SO_2
3	− 68 to 10	H_2O

are reported to occur between 130 and 200 °C and would account for an increase in water from 0.035 to 0.11 mbar in the isothermal SAD curve at 190 °C (Fig. 8) and the presence of CO_2 in the mass spectrum (Fig. 7).

From 190 to 275 °C, sufficient pressure has been produced within the graphite layers to break the Van der Waals attractions and allow expansion to occur along the *c*-axis. In the isothermal TVA curve at 275 °C, a small volume of non-condensable products is detected, another indication that the TEG is a combination of both graphite bisulfate and graphite oxide. Graphite oxide has been reported to contain epoxide, carboxyl, and other carbonyl groups, which when subjected to heat are released. As CO_2 and CO are both observed at 275 °C, it is proposed that functional groups

such as carboxylic acids, carbonyls, and epoxides produced during oxidation decompose under thermal conditions. Therefore, it is the decomposition of these CO-containing functional groups which are responsible for expansion rather than SO_2, which is only observed in trace quantities at this temperature (Fig. 8).

By 275 °C, the main expansion step has plateaued; however, volatile products are still forming. At 575 °C, a large peak at − 101 °C appears in the SAD curve, confirmed by MS and FTIR to predominately consist of SO_2. The largest volume of CO_2 is also recorded at this stage suggesting subsequent reactions are occurring above exfoliation temperatures. This is proposed to be due to the release of free sulfuric acid previously embedded within the layers, which at around 340 °C has been reported to thermally decompose to SO_3 and H_2O. This also corresponds to the onset of volatile evolution for peak 3 in the dynamic TVA experiment (Fig. 1). Free SO_3 decomposes at temperatures above 450 °C, and this decomposition in the presence of carbon may occur via reaction 10 [8]:

$$3C + 4SO_3 \rightarrow S + 3CO_2 + 3SO_2 \tag{10}$$
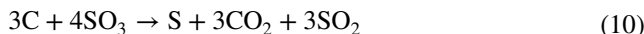
This reaction may therefore account for the formation of SO_2 and increased volumes of CO_2 at higher temperatures. Furthermore, SO_2 produced in the first stage of the reaction may functionalise the surface and edges of graphite. It is possible that along with CO-containing functional groups, thiol and sulfonic acid groups are created from interactions with carbon and SO_2 produced in the first stage of the reaction. Weng et al. [28] showed that SO_2 may interact with epoxy groups on the surface of graphite powder creating $C\text{-}O\text{-}SO_3H$. These types of functional groups have been shown to decompose to release SO_3 from around 268 °C [29].

Analysis of the data reveals three key events in the mechanism of action of expandable graphite: the desorption of gases leading to increased d-spacing, then, consequently, the removal of the Van der Waals attractions causing exfoliation along the *c*-axis, and finally, the decomposition of de-intercalated products.. The schematic diagram in Fig. 9 shows the process of exfoliation in relation to the dynamic TVA curve.

Thermal expansion of graphite nitrate

Dynamic thermal volatilisation analysis

The dynamic TVA profile (Fig. 10) shows the volatile release profile associated with the thermal expansion of graphite nitrate under vacuum as a function of furnace temperature.
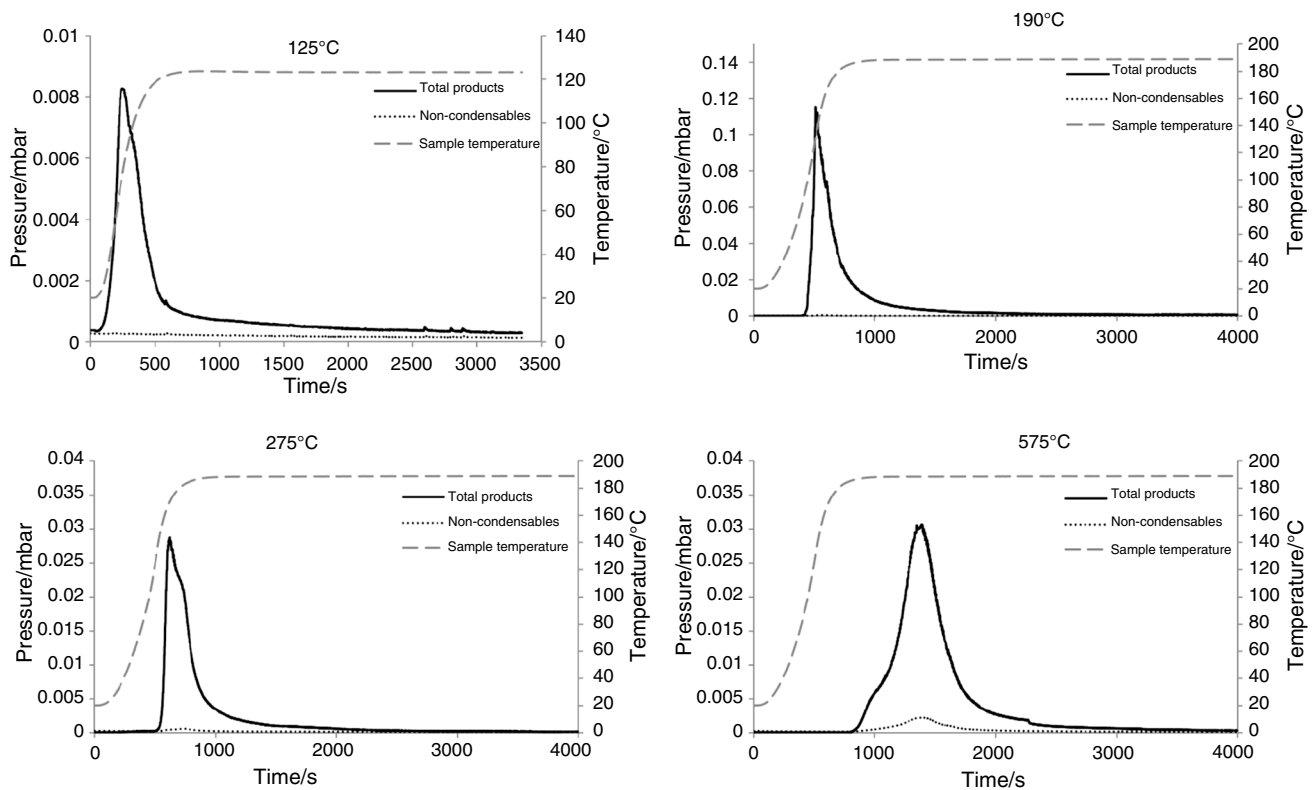
Fig. 6 Isothermal TVA degradation profiles for graphite bisulfate at 120, 190, 275 and 575 °C

Table 3 Characterisation of products from isothermal TVA experiments for graphite bisulfate

Degradation temperature /°C	Volatile products
125	CO_2 and H_2O
190	CO_2, SO_2 (trace), and H_2O
275	CO_2, SO_2 (trace), H_2O, and CO
575	CO_2, SO_2, H_2O, and CO

The sample temperatures for each key thermal event are summarised in Table 4.

The TVA curve from the dynamic run of graphite nitrate shows three main peaks of volatile evolutions. According to Saidaminov et al. [11], graphite nitrate ($4C_{24n}^+ NO_3^-.xHNO_3$) can be expected to decompose with the release of CO, CO_2, NO, NO_2, and water by the following reactions:

$$4C_{24n}^+NO_3^-.xHNO_3 \rightarrow 96nC + (4 + 4x)NO_2 + 5O_2 + 6H_2O \tag{11}$$
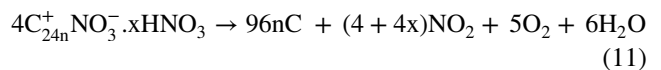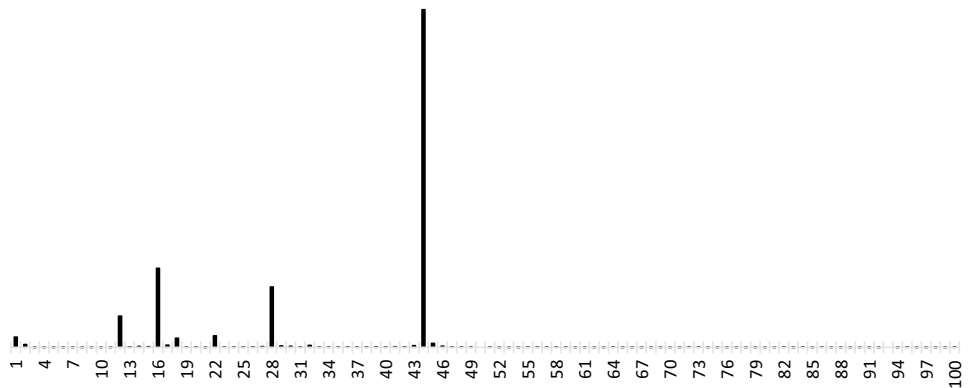
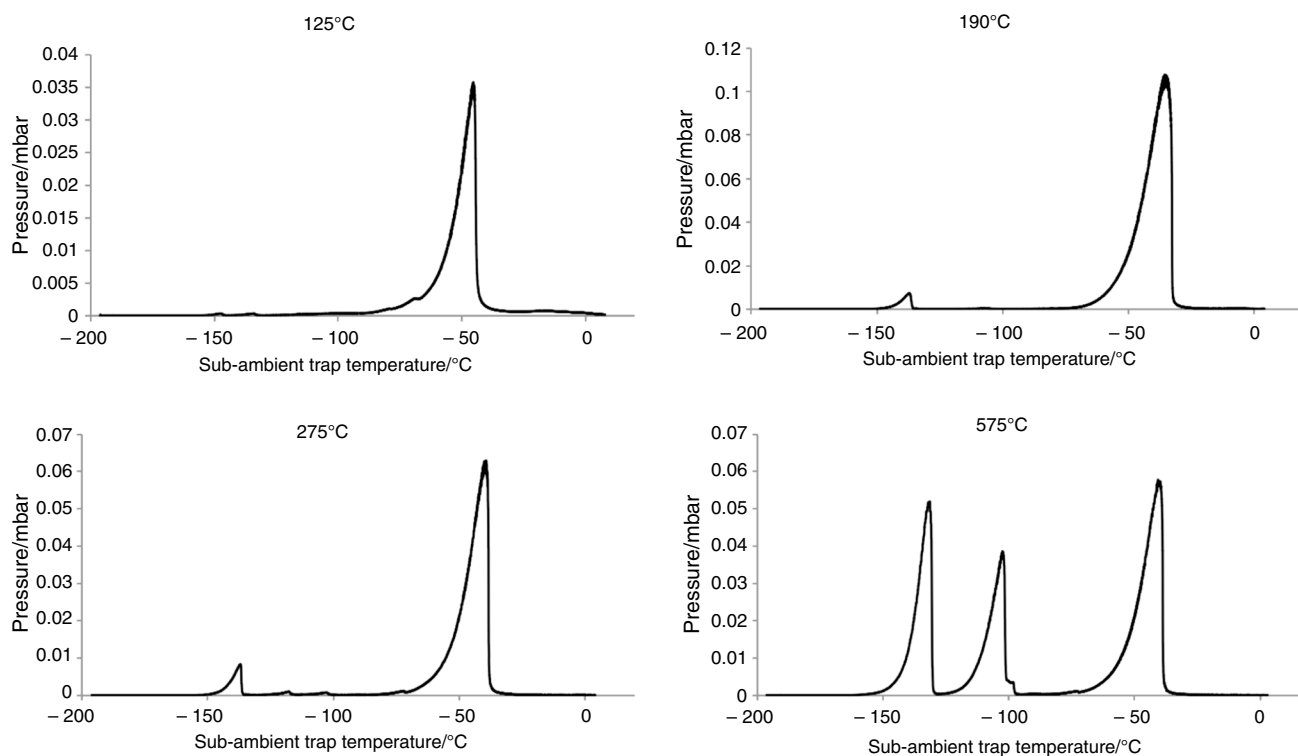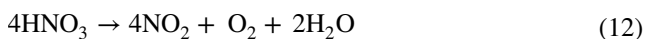**Fig. 7** MS of CO_2 collected from the isothermal TVA experiment at 190 °C

Fig. 8 SAD curves for the condensable fractions collected from graphite bisulfate upon isothermal heating at 125, 190, 275, and 575 °C

$$4HNO_3 \rightarrow 4NO_2 + O_2 + 2H_2O \qquad (12)$$

$$C + O_2 \rightarrow CO_2 \qquad (13)$$

$$2C + O_2 \rightarrow 2CO \qquad (14)$$

$$C + NO_2 \rightarrow CO + NO \qquad (15)$$

The curve indicates a maximum evolution of volatiles around 150 °C which correlates to the onset temperature of exfoliation for graphite nitrate quoted in the literature. This marks the start of expansion which is mostly complete by 350 °C. Non-condensable products observed around 90 °C are thought to be a consequence of CO produced in the above reactions and the decomposition of carbonyl-containing functional groups created by oxidation of graphite. The largest volume of non-condensable material is produced at a peak maximum of 405 °C suggesting other degradation reactions are occurring past the point of total exfoliation. To fully characterise these individual processes, the sub-ambient fractions must be examined.

Sub-ambient distillation and characterisation

The sub-ambient curve for the dynamic TVA experiment for graphite nitrate is presented in Fig. 11. Characterisation

of products was carried out by FTIR and MS, the identifications for each peak are presented in Table 5 and FTIR spectra are displayed in Fig. 12.

Four main products were collected in the SAD analysis: CO_2, NO and NO_2, and H_2O. Reactions 11 and 12 above demonstrate that H_2O is a major decomposition product, resulting from the initial decomposition of graphite nitrate and subsequent decomposition reactions thereof. CO_2 can also be expected as the result of the reaction with O_2, formed from the decomposition of HNO_3 and carbon.

Isothermal thermal volatilisation analysis

Isothermal experiments were performed to capture the volatiles produced from each main thermal event. TVA and SAD curves are presented in Figs. 13 and 15 respectively.

Sequential isothermal analyses were conducted at 145, 245, 350, and 575 °C. Products were separated into two to three fractions and then characterised by MS and FTIR. Product identification is presented in Table 6.

The TVA curve at 145 °C represents the first stage in graphite nitrate exfoliation which encompasses the desorption of migrating intercalated molecules and the decomposition of HNO_3, which occurs around 82 °C to produce NO_2, and H_2O.

From 145 °C to around 245 °C, the graphite nitrate begins to expand rapidly accompanied by the release of
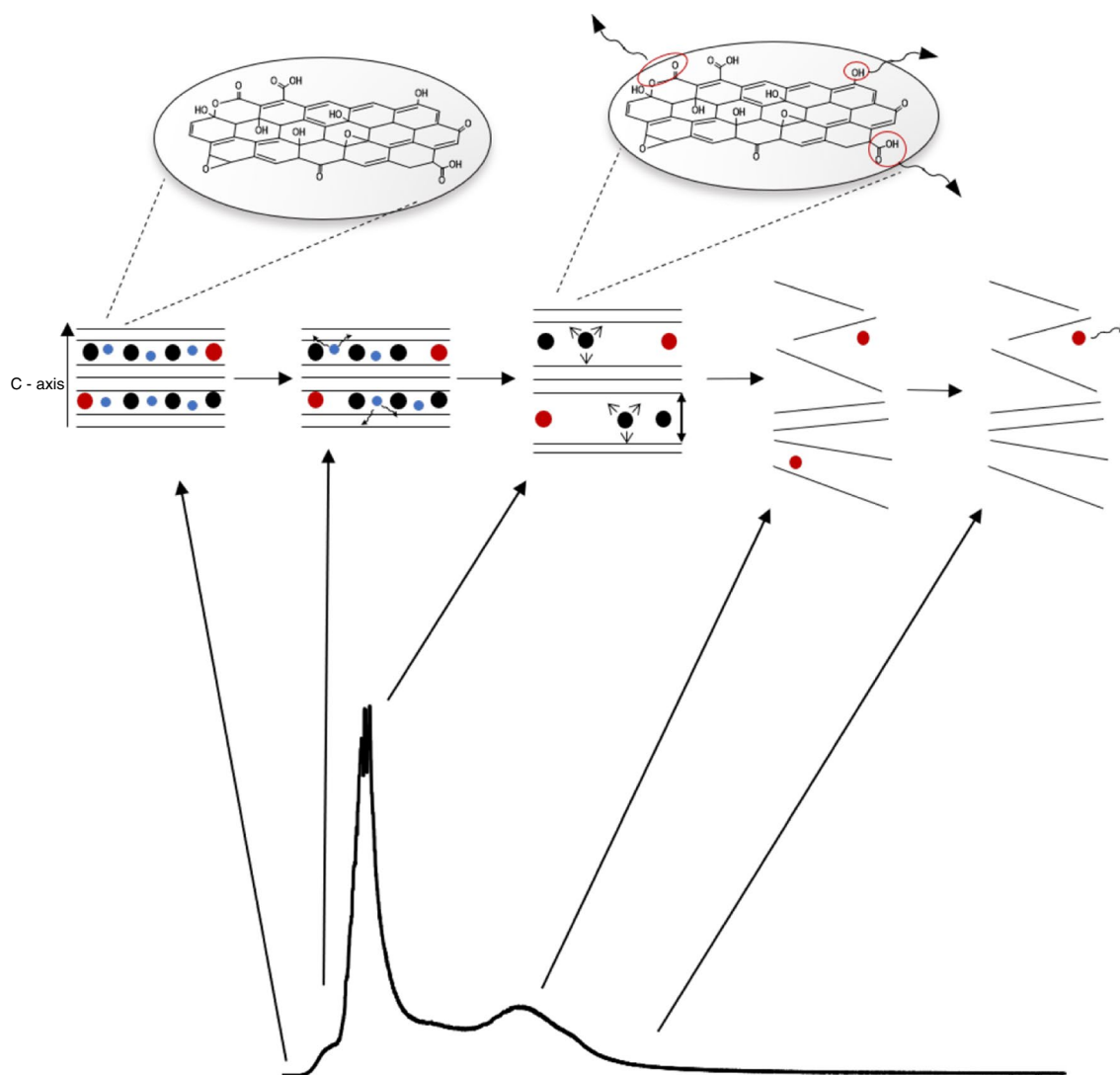
Fig. 9 A schematic representation of the expansion of GIC graphite bisulfate in relation to TVA, showing the initial evaporation of water (blue dots), followed by an increase in d-spacing due to the evaporation and decomposition of CO-containing functional groups and vola-tile products (black dots). Finally, expansion along the c-axis as Van der Waals attractions are broken and free H_2SO_4 (red dots) decomposes resulting in a thermally stable char

non-condensable species. This may be due to further oxidation reactions occurring between carbon and O_2 generated from the decomposition of HNO_3.

The TVA curves again at 350 and 575 °C are accompanied by the presence of non-condensable products. At this stage, although all noticeable expansion has occurred, volatiles are still being produced. To further examine the degradation chemistry, the sub-ambient products can be studied.

Isothermal Sub-ambient distillation and characterisation

At 145 ˚C, the major volatiles species produced in the first stage of graphite nitrate exfoliation are confirmed by MS and FTIR to be CO_2 and H_2O with trace quantities of HCl and H_2SO_4. Trace amounts of H_2SO_4 and HCl suggest these acids were used as part of the preparation procedure, most likely as an assistant intercalation agent in the case of H_2SO_4 and as part of the final washing process for HCl. A large volume of water may be expected due to the evaporation of residual water from the washing stage during intercalation and the desorption of intercalated molecules. Water has also been reported to evolve in the first decomposition stage of graphite oxide degradation from 80 °C. This can account for large volumes of water in the FTIR and MS spectra.

The SAD curve for the condensable products collected upon the isothermal degradation at 245 °C shows a large increase in the evolution of volatiles between − 125 and

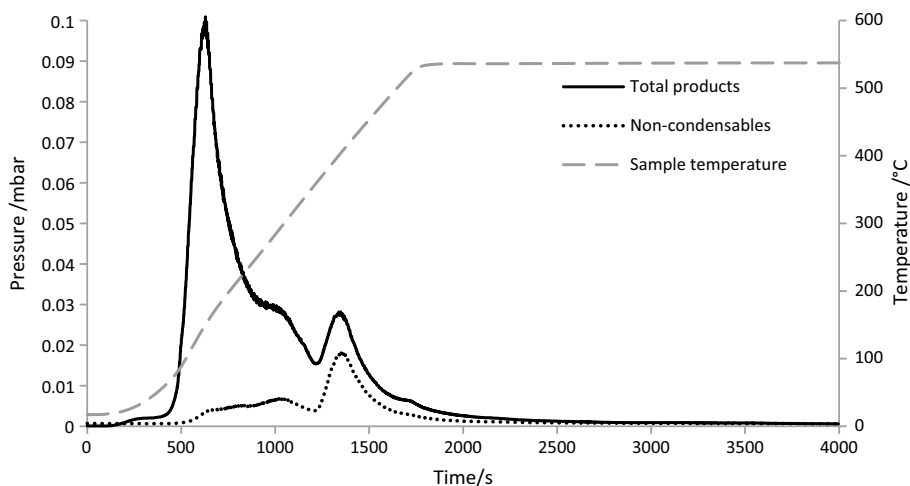**Fig. 10** Dynamic TVA degradation profile for the thermal expansion of graphite nitrate

Table 4 Temperatures for the main thermal events occurring in the expansion process for graphite nitrate

Degradation peak	Onset of evolution of volatiles /°C	Maximum evolution of volatiles /°C	End of volatile evolution /°C
Peak 1	65	150	245
Peak 2	245	297	350
Peak 3	350	405	535

− 76 °C. These are identified by MS and FTIR to be a mixture of NO and NO_2 and HNO_3. Products at this temperature correlate with the decomposition of NO_2 to O_2 and NO which occurs at 160 °C and are also consistent with the thermal decomposition of nitric acid by reaction 12.

The pressure recorded by the Pirani gauges during the isothermal at 245 °C is at the maximum detected during analysis. This correlates with the rapid expansion of graphite from around 150 °C as Van der Waals attractions are broken and the graphite layers are pushed apart. This is likely to be
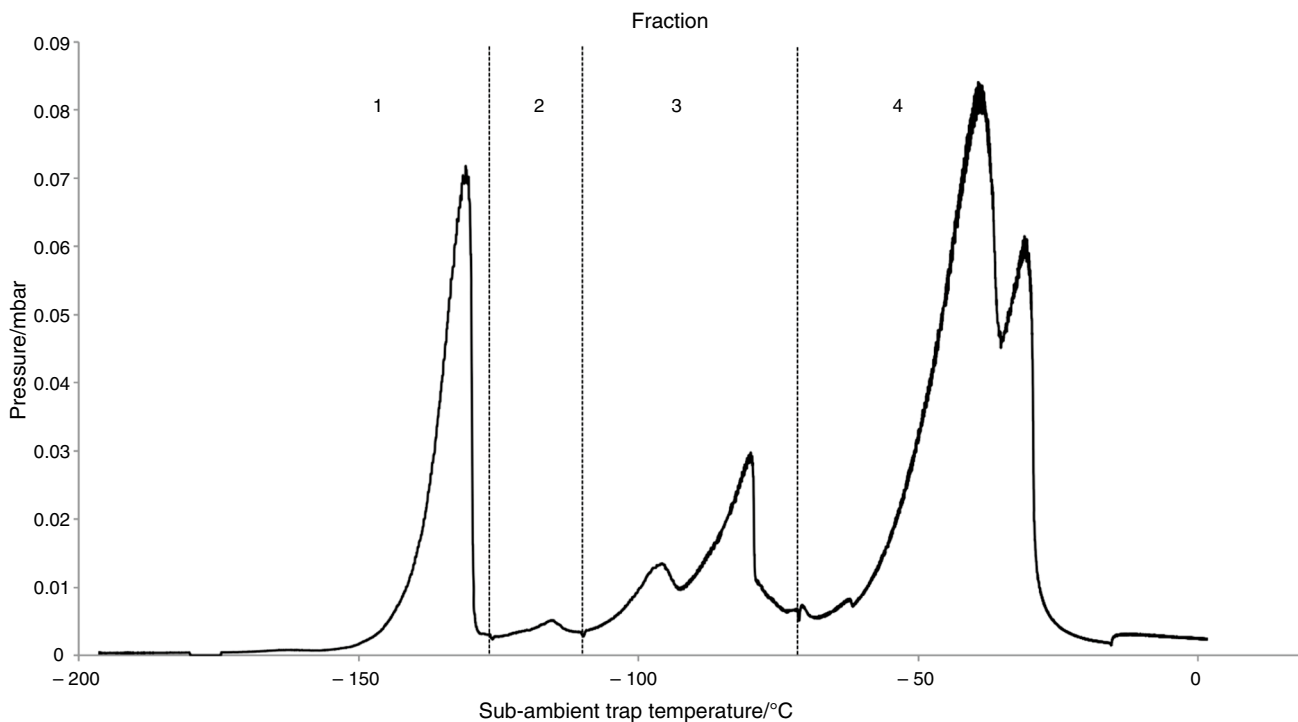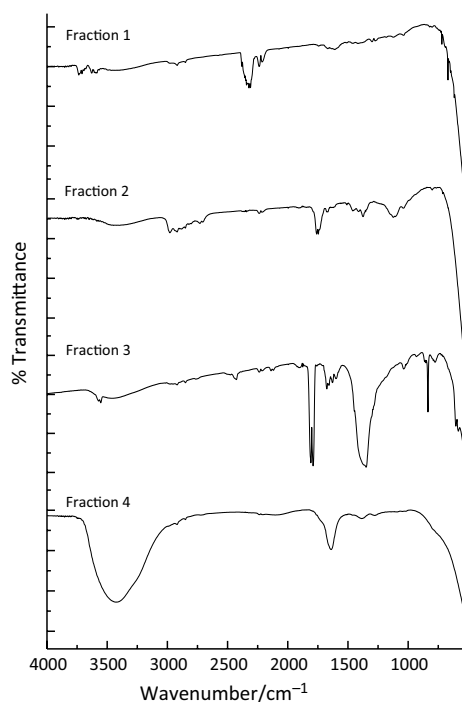

Fig. 11 SAD curve for the condensable fraction collected from the dynamic TVA run for graphite nitrate

**Table 5** Characterisation of products from the dynamic TVA run for graphite nitrate

Fraction	Fraction range /°C	Condensable products
1	− 200 to − 125	CO_2
2	− 125 to − 110	NO, H_2SO_4 (trace)
3	− 110 to − 71	NO, NO_2, HNO_3 (trace)
4	− 71 to + 5	H_2O, HCl (trace)

Fig. 12 FTIR gas phase spectra of the volatile SAD products in fractions 1—4 from the dynamic TVA for graphite nitrate showing CO_2 (fraction 1), NO (fraction 2), NO, NO_2, and HNO_3 (fraction 3), and H_2O (fraction 4)

attributed to the decomposition of intercalated HNO_3 and NO_3^- and their decomposition products as shown in reaction 12. The positively charged graphite can then undergo further oxidation creating areas of graphite oxide type material. This may occur similarly to graphite bisulfate by oxidation of the flaws in graphite creating pockets of trapped gas.

It is also interesting to note the presence of a blue material condensed in the FTIR gas cells in fractions 2 and 3. This may be due to the reaction between generated NO_2 and water. As NO_2 and N_2O_4 exist in equilibrium, both products are likely to be present.

When water is in contact with N_2O_4, dinitrogen trioxide may also be formed in the reaction:

$$2N_2O_4 + H_2O \rightarrow 2N_2O_3 + 2HNO_3 \tag{16}$$
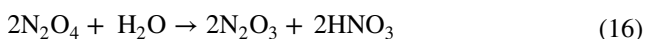
N_2O_3 is a blue liquid at temperatures below -101 °C, which may account for the observation of a blue material in the gas cell at low temperatures. FTIR analysis (Fig. 14) also confirms several absorptions expected from the equilibrium mixture of NO_2/N_2O_4.

During the exfoliation process, there is a large increase in H_2O and CO_2 evolution and non-condensable species are observed in the TVA curve. Further oxidation of graphite may have occurred because of reactions between oxygen created in the decomposition of nitric acid and the graphite. Therefore, similarly to graphite bisulfate, there may be highly oxidised areas within the structure that decompose and contribute to exfoliation. It has been reported that oxidation of graphite to graphite oxide occurs readily when treated with nitric acid. This results in the formation of epoxy and hydroxyl functional groups in between layers and carbonyl, anhydride, and carboxylic groups on the periphery. Acid anhydrides, lactols, and ketones have also been reported in structural studies of graphite oxide [30]. During heat treatment, some of these oxygen-containing functional groups are removed, particularly those on the outer edges.

At 350 °C, the condensable products collected are identical to those collected at 245 °C according to FTIR and MS analysis, only at lower volumes. As intercalated NO_3^- anions are released from the graphitic structure due to NO_2 decomposition, they may also decompose releasing NO_2 and O_2:

$$NO_3 \rightarrow NO_2 + O \tag{17}$$

$$NO_3 \rightarrow NO + O_2 \tag{18}$$

This decomposition can be observed on the TVA curve marked by an increase in pressure as volatile products are released. As the evolution of volatiles at this stage is present as a shoulder on the principal peak observed in the dynamic TVA curve (Fig. 10), NO_2 decomposition and HNO_3 decomposition are likely to be overlapping processes. A slight increase in non-condensable products may be a consequence of the decomposition of carbonyl-containing groups previously dissociated from the graphene structure to yield CO.

The final isothermal analysis accounts for the peak with a maximum evolution of volatiles at 400 °C. It can be observed in the dynamic experiment (Fig. 10) that this is predominately composed of non-condensable species. It is therefore probable that CO is being released from the system due to the reaction between generated oxygen and carbon and as a decomposition product of graphite oxide. Additionally, carbonyl functional groups created from the oxidation of graphite, which are sensitive to high temperatures, may contribute to the non-condensable species as they decompose producing CO.

The final isothermal experiment exposed the graphite nitrate to a maximum temperature of 575 °C, by this stage,
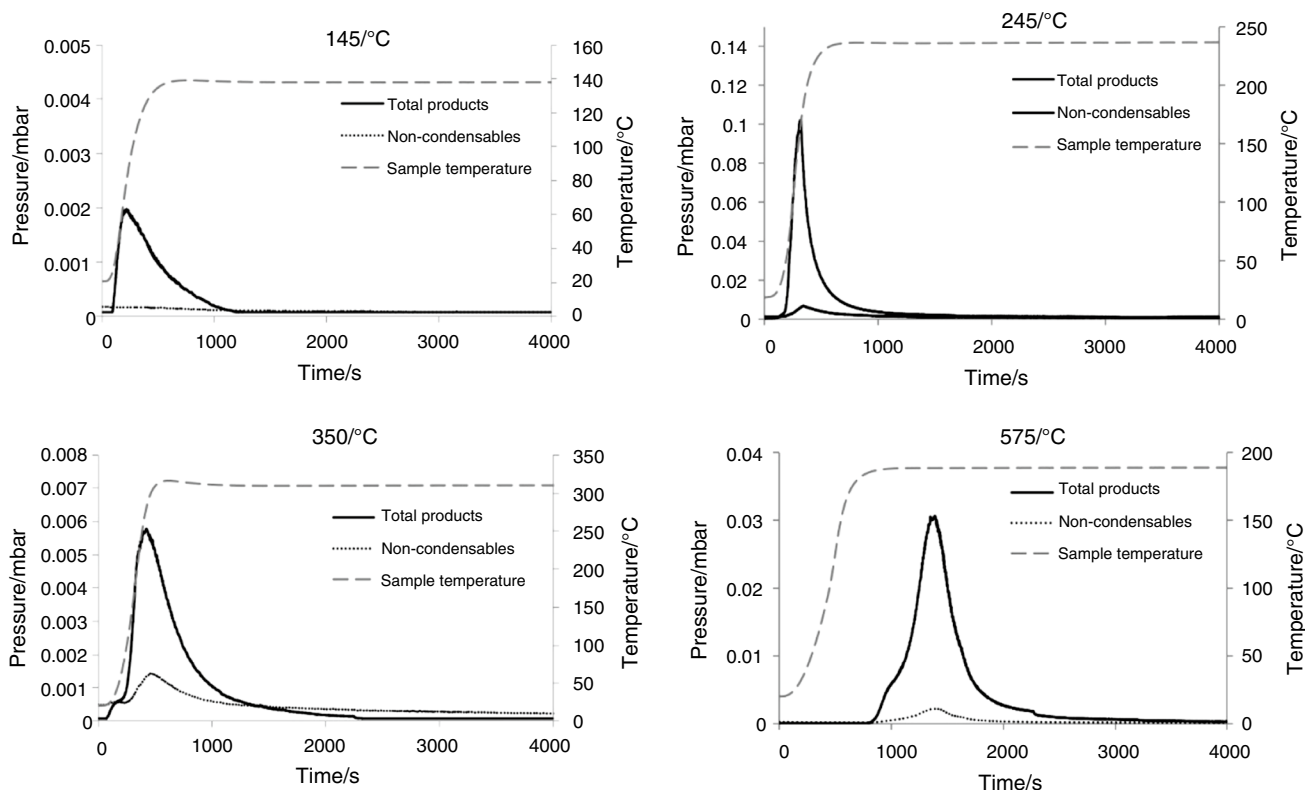
Fig. 13 Isothermal TVA degradation profiles for graphite nitrate at 145, 245, 350, and 575 °C

Table 6 Characterisation of products from isothermal TVA experiments for graphite nitrate

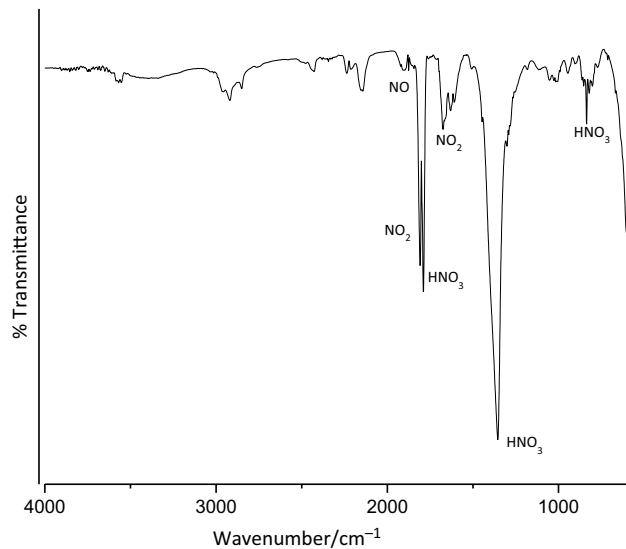| Degradation temperature /°C	Volatile products
145	CO_2, H_2SO_4 (trace), HCl (trace), H_2O,
245	CO
350	CO_2, NO, NO_2/N_2O_4, HNO_3 (trace)
575	H_2O, CO
	CO_2, NO, NO_2/N_2O_4
	H_2O, H_2SO_4 (trace), CO
	CO_2, NO, H_2O, CO

Fig. 14 FTIR spectrum of the volatile SAD products in fraction 2 from the isothermal TVA at 245 °C (?) for graphite nitrate showing absorptions of NO_2/N_2O_4 and HNO_3

it is apparent that all NO_2 has decomposed as it is no longer visible in MS and FTIR spectra. Similarly, nitric acid is not observed in the FTIR spectra at temperatures above 350 °C (Fig. 16) verifying it has decomposed predominantly during the exfoliation process and is no longer producing NO_2, CO_2, NO, and H_2O are still however being produced in similar quantities indicating that intercalated anions may still be present and continue to decompose.
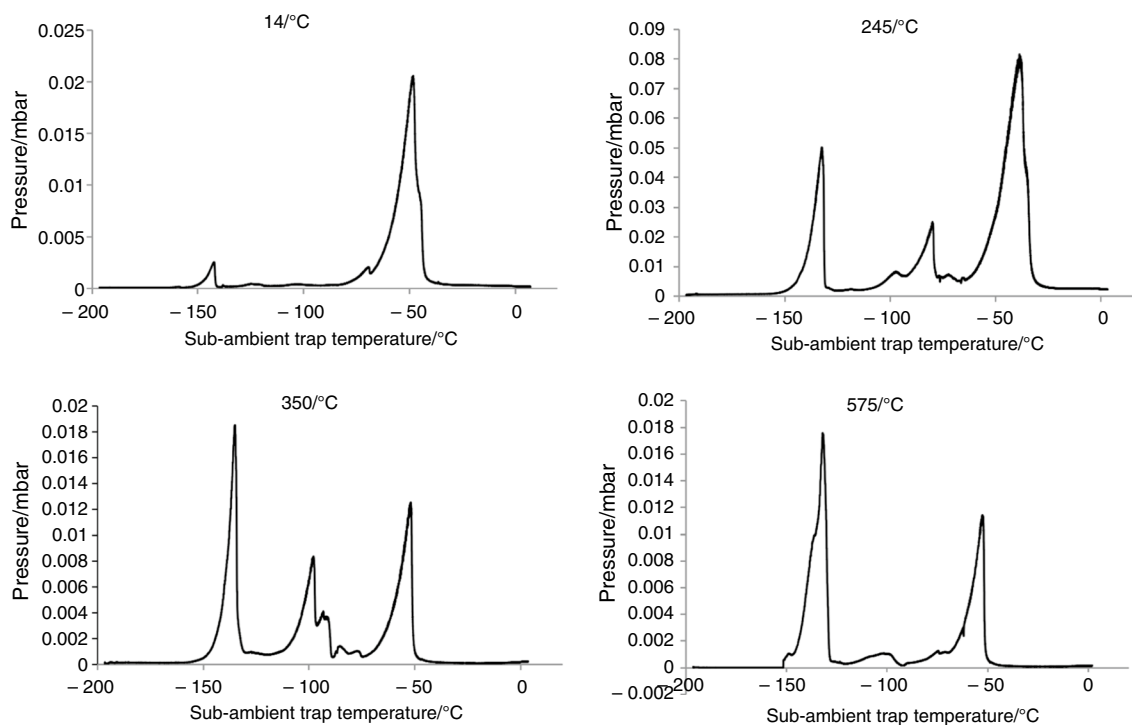
Fig. 15 SAD curves for the condensable fractions collected from graphite nitrate upon isothermal heating at 145, 245, 350 and 575 °C
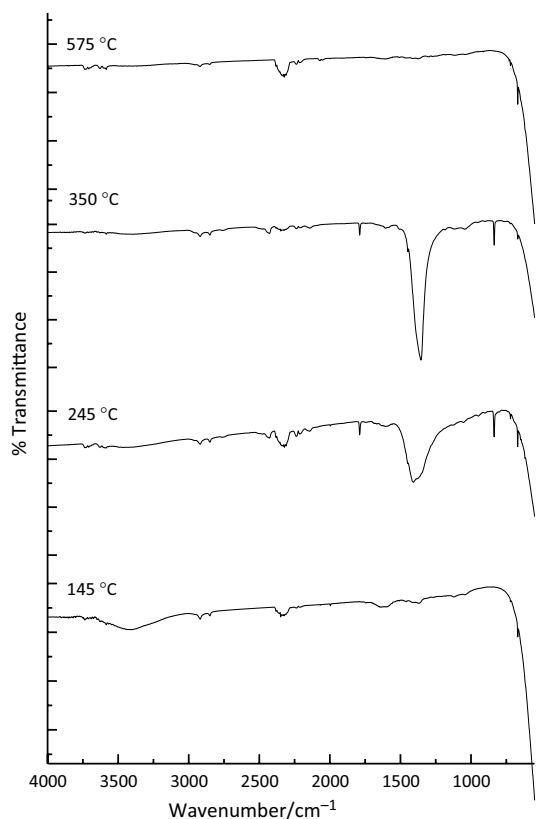

Fig. 16 FTIR spectra from fraction 1 of gases collected from the isothermal experiments showing CO_2 (145 and 575 °C) and HNO_3 (245 and 350 °C)

Conclusions

In conclusion, thermal volatilisation analyses were performed on two commercially available GICs, one containing intercalated nitric acid and the other sulfuric acid. The thermal decomposition was found to be a complex process in both instances whereby a combination of processes results in the generation of SO_2, CO_2, CO, and H_2O for graphite bisulfate and NO_2, NO, CO, CO_2, and H_2O for graphite nitrate.

It is evident from the TVA curves that the thermal decomposition proceeds with three main thermal events, the desorption of gases, exfoliation, and then the decomposition of de-intercalated products.

The data obtained from the isothermal analyses provided an in-depth characterisation of products that evolved at each thermal event. For both graphite bisulfate and graphite nitrate, the main exfoliation event proceeds with the evolution of non-condensable species and CO-derived fragments. It is therefore assumed that exfoliation is partially attributed to the decomposition of oxidised graphite to create carbonyl, carboxy, epoxide, and other CO groups which when subjected to heat thermally decompose releasing CO, CO_2, and water. The vaporisation of these intercalated species combined with the decomposition of the acids and anions ultimately results in enough pressure required to break the Van der Waals attractions and cause expansion. For graphite bisulfate, significant volumes of SO_2 are produced only at

temperatures beyond expansion, suggesting that it does not play a vital role in the expansion as initially anticipated.

In the case of graphite nitrate, the peak maximum exfoliation temperature is 150 °C, compared to 190 °C for graphite bisulfate, and it is the decomposition of intercalated HNO_3 and NO_3^- to NO_2, H_2O, and O_2 that creates enough pressure to initially break Van der Waals attractions and rupture the graphitic structure. It can be noted by the presence of a shoulder on the TVA trace that expansion is an overlapping process suggesting a combination of thermal events are occurring. This may be the consequence of further reactions from intercalated anions as they are released from the graphite layers, releasing O_2 and oxidising areas of the graphite. Further oxidation of the graphite in the expansion process can be noted by an increase in CO past 350 °C.

Overall, thermal volatilisation analysis has provided valuable information in order to understand the mechanistic detail and capture volatile degradation products released from the thermal exfoliation of two GICs. A mechanism of action has been proposed in which evaporation of intercalated water and decomposition of CO-containing functional groups are responsible for the expansion of graphite bisulfate but play a lesser role in the expansion of graphite nitrate which is predominantly due to the volatilisation of intercalated acid and acidic anions.

Author contribution All three authors contributed to the study conception and design. Material preparation, data collection and analysis were performed by KM. The first draft of the manuscript was written by KM, and all three authors commented on previous versions of the manuscript. All three authors read and approved the final manuscript.

Data availability The data required to reproduce these findings are available to download from https://doi.org/10.15129/1e3327e0-cc16-49ea-a67c-2ab170bc4479

Declarations

Conflict of interest The work reported in this manuscript forms part of the PhD research of the first author, Kellie Muir, supervised by John Liggat. The PhD studentship was funded by Abesco Fire Ltd (UK company number 08048304) of which Luke O'Keeffe is a director.

References

1. Celzard A, Marêché JF, Furdin G. Modelling of exfoliated graphite. Prog Mater Sci. 2005. https://doi.org/10.1016/j.pmatsci.2004.01.001.

2. Cai M, Thorpe D, Adamson DH, Schniepp HC. Methods of graphite exfoliation. J Mater Chem. 2012. https://doi.org/10.1039/C2JM34517J.

3. Alongi J, Han Z, Bourbigot S. Intumescence: tradition versus novelty. A Compr Rev Prog Polym. 2015. https://doi.org/10.1016/j.progpolymsci.2015.04.010.

4. Gharehbaghi A, Bashirzadeh R, Ahmadi Z. Polyurethane flexible foam fire resisting by melamine and expandable graphite: industrial approach. J Cell Plast. 2011. https://doi.org/10.1177/0021955X11414789.

5. Modesti M, Lorenzetti A, Simioni F, Camino G. Expandable graphite as an intumescent flame retardant in polyisocyanurate-polyurethane foams. Polym Degrad Stab. 2002. https://doi.org/10.1016/S0141-3910(02)00034-4.

6. Duquesne S, Le Bras M, Bourbigot S, Delobel R, Vezin H, Camino G, Eling B, Lindsay C, Roels T. Expandable graphite: a fire retardant additive for polyurethane coatings. Fire Mater. 2003. https://doi.org/10.1002/fam.812.

7. Wang X, Wang G, Zhang L. Green and simple production of graphite intercalation compound used sodium bicarbonate as intercalation agent. BMC Chem. 2022. https://doi.org/10.1186/s13065-022-00808-y.

8. Furdin G. Exfoliation process and elaboration of new carbonaceous materials. Fuel. 1998. https://doi.org/10.1016/S0016-2361(97)00142-7.

9. Chung DDL, Anderson Axdal SH. A theory for the kinetics of intercalation of graphite. Carbon. 1987. https://doi.org/10.1016/0008-6223(87)90009-1.

10. Dreyer DR, Park S, Bielawski CW, Ruoff RS. The chemistry of graphene oxide. Chem Soc Rev. 2010. https://doi.org/10.1039/B917103G.

11. Saidaminov MI, Maksimova NV, Zatonskih PV, Komarov AD, Lutfullin MA, Sorokina NE, Avdeev VV. Thermal decomposition of graphite nitrate. Carbon. 2013. https://doi.org/10.1016/j.carbon.2013.03.028.

12. Forsman WC, Vogel FL, Carl DE, Hoffman J. Chemistry of graphite intercalation by nitric acid. Carbon. 1978. https://doi.org/10.1016/0008-6223(78)90040-4.

13. Duquesne S, Le Bras M, Bourbigot S, Delobel R, Poutch F, Camino G, Eling B, Lindsay C, Roels T. Analysis of fire gases released from polyurethane and fire-retarded polyurethane coatings. J Fire Sci. 2000. https://doi.org/10.1106/6CRG-Q8VD-PV3G-ELD.

14. Hofmann U, Rudorff W. The formation of salts from graphite. Trans Faraday Soc. 1938. https://doi.org/10.1039/TF9383401017.

15. Chung DDL. Review exfoliation of graphite. J Mater Sci. 1987. https://doi.org/10.1007/BF01132008.

16. Camino G, Duquesne S, Delobel R, Eling B, Lindsay C, Roels T. Mechanism of expandable graphite fire retardant action in polyurethanes. In: Nelson GL, Wilkie CA, editors. Fire and polymers: materials and solutions for hazard prevention. Washington: American Chemical Society; 2001. p. 90–109. https://doi.org/10.1021/bk-2001-0797.ch008.

17. Focke WW, Badenhorst H, Mhike W, Kruger JH, Lombaard D. Characterization of commercial expandable graphite fire retardants. Thermochim Acta. 2014. https://doi.org/10.1016/j.tca.2014.03.021.

18. Sofer Z, Jankovský O, Šimek P, Sedmidubský D, Šturala J, Kosina J, Mikšová R, Macková A, Mikulics M, Pumera M. Insight into the mechanism of the thermal reduction of graphite oxide :

deuterium-labeled graphite oxide Is the key. ACS Nano. 2015. https://doi.org/10.1021/acsnano.5b01463.

19. Peng T, Liu B, Gao X, Luo L, Sun H. Preparation, quantitative surface analysis, intercalation characteristics and industrial implications of low temperature expandable graphite. App Surf Sci. 2018. https://doi.org/10.1016/j.apsusc.2018.03.089.

20. Cirmad H, Tirkes S, Tayfun U. Evaluation of flammability, thermal stability and mechanical behaviour of expandable graphite-reinforced acrylonitrile–butadiene–styrene terpolymer. J Therm Anal Calorim. 2022. https://doi.org/10.1007/s10973-021-10656-y.

21. Wang Y, Wang F, Dong Q, Xie M, Liu P, Ding Y, Zhang S, Yang M, Zheng G. Core-shell expandable graphite @ aluminum hydroxide as a flame-retardant for rigid polyurethane foams. Polym Deg Stab. 2017. https://doi.org/10.1016/j.polymdegradstab.2017.10.017.

22. Ning H, Ma Z, Zhang Z, Zhang D, Wang Y. Core–shell expandable graphite @ layered double hydroxide as a flame retardant for polyvinyl alcohol. J Therm Anal Calorim. 2022;147:6249–58. https://doi.org/10.1007/s10973-021-10843-x.

23. Pan Y, Yin C, Fernandez C, Fu L, Lin C-T. A systematic review and bibliometric analysis of flame-retardant rigid polyurethane foam from 1963 to 2021. Polymers. 2022. https://doi.org/10.3390/polym14153011.

24. McNeill IC. Thermal volatilization analysis: a new method for the characterization of polymers and the study of polymer degradation. J Polym Sci. 1966. https://doi.org/10.1002/pol.1966.150041012.

25. Schwartz D, Gadiou R, Prado G, Martinez G. A kinetic study of the decomposition of spent sulfuric acids at high temperature. Ind Eng Chem Res. 2000. https://doi.org/10.1021/ie990801e.

26. Valerga Jimenez PS. Thermal decomposition of graphite oxidation products DSC studies of internal combustion of graphite oxide. Mat Res Bull. 1987. https://doi.org/10.1016/0025-5408(87)90108-5.

27. Yakovlev AV, Finaenov AI, Zabud'kov SL, Yakovleva EV. Thermally expanded graphite: synthesis, properties, and prospects for use. Russ J Appl Chem. 2006. https://doi.org/10.1134/S1070427206110012.

28. Xie W, Weng L-T, Chan C-K, Yeung KL, Chan C-M. Reactions of SO_2 and NH_3 with epoxy groups on the surface of graphite oxide powder. Phys Chem Chem Phys. 2018. https://doi.org/10.1039/C8CP00524A.

29. Liu F, Sun J, Zhu L, Meng X, Qi C, Xiao F-S. Sulfated graphene as an efficient solid catalyst for acid-catalyzed liquid reactions. J Mater Chem. 2012. https://doi.org/10.1039/C2JM16608A.

30. Gao W, Alemany LB, Ci L, Ajayan PM. New insights into the structure and reduction of graphite oxide. Nat Chem. 2009. https://doi.org/10.1038/nchem.281.